Experimental Thermal and Fluid Science 38 (2012) 14–18

Contents lists available at SciVerse ScienceDirect

Experimental Thermal and Fluid Science

journal homepage: www.elsevier.com/locate/etfs

A measurement of light absorption using an image-based technique

Jeonghoon Lee [a,*], Jung Kyung Kim [b]

[a] School of Mechanical Engineering, Korea University of Technology and Education, Cheon An 330-708, Republic of Korea
[b] School of Mechanical Engineering, Kookmin University, Seoul 136-702, Republic of Korea

ARTICLE INFO

Article history:
Received 22 April 2011
Received in revised form 2 August 2011
Accepted 29 October 2011
Available online 13 December 2011

Keywords:
Absorbing particle
Interferometry
Spherical particle

ABSTRACT

In the present study, absorption coefficients were measured by an image-based photothermal technique. Spherical absorbing particles were generated using an atomizer, which produced a constant number of particles. Phase shifts were measured by image analysis of interference patterns created at which two split coherent beams were recombined. Our preliminary results show that light absorptions from particles were quantified during a short term.

1. Introduction

Various instruments have been used for measuring the light absorption of particles and gas species. For example, a photoacoustic spectroscopy (PAS) has been utilized for measuring the light absorption of particles; PAS instrument has been considered as an advanced tool for such measurements. The PAS instrument was already commercialized and various research groups are using that for the purpose of measuring light absorption. A recent study conducted by Moosmüller et al. presents light absorption by aerosols and various measurement techniques including PAS [1]. Photoacoustic spectrometers detect sound waves created from a sample heated by a modulated optical power source such as a laser. The sound waves which are detected by microphones are converted to light absorption coefficient by calibration. A photothermal interferometer employs an experimental setup similar to that of the PAS but in contrast to the PAS, detects the changes in the refractive index of air surrounding the particle sample. Photothermal interferometric technique was utilized for measuring the absorption of aerosol particles as well as a gas species [2,3]. Photothermal technique was also used to measure thermal properties even for thin films due to its high sensitivity [4].

Not only the PAS and the photothermal interferometer but also filter-based techniques are used to measure the light absorption from particles. A particle soot absorption photometer (PSAP) measures the light absorption of aerosol particles [5]. The PSAP is a filter-based instrument that measures the difference of transmittance after the deposition of aerosols onto a filter. A multi angle absorption photometer (MAAP) also measures the light absorption of particles with algorithms for correcting the effect of scattering, which always amplifies the absorption level [6]. An aethalometer was used to determine the absorption of light by soot particles [7]. The aethalometer measures optical absorption in real time with one or two wavelengths using the filter deposition and the optical attenuation method.

Soot particles are typically generated through flame combustion in automotive engines and power plants. Biomass burning is also one of causes of soot particle generation. The soot particles existing in the atmosphere absorb light and dissipate the absorbed energy toward the atmosphere. The soot particles include carbonaceous particles such as black carbon (BC). BC attracts great attention since a small mass fraction of BC may contribute the equivalent of 1/4 of radiative forcing caused by CO_2 [8]. More recently, it has been reported that the BC forcing could even be as much as 55% of the CO_2 forcing [9]. The BC forcing should be correctly assessed by a more reliable measurement technique. Optical method (PAS, photothermal interferometer) rather than the filter-based technique is recommended to measure the absorption coefficient since the sensitivity for the optical method is better. An image-based method with a Mach–Zehnder interferometric configuration is used as a tool for measuring the optical properties of absorbing particles. Photothermal interferometric technique as in the case of the PAS allows for a direct measurement of absorption property. In addition, scattering does not contribute to the absorption, thus the absorption property is not affected by the scattering. The photothermal interferometer used in the present study consists of affordable optical components and does not require digital signal processing instruments such as a lock-in amplifier during a short term experiment. Thus, conducting this research at a relatively low-cost was possible.

* Corresponding author.
E-mail address: jlee@kut.ac.kr (J. Lee).

0894-1777/$ - see front matter © 2011 Elsevier Inc. All rights reserved.
doi:10.1016/j.expthermflusci.2011.10.016

2. Method

The photothermal interferometric technique measures changes in the optical path length of the probe beam relative to the reference beam when an aerosol sample surrounding the probe beam is thermally heated [10]. An interference pattern was created when the two split beams were recombined at a beamsplitter. The interference pattern will change if the optical path length of the probe beam changes. Interferometry allows us to detect the changes because of its precision and accuracy. Interferometry facilitates the realization of the SI meter. The change in the interference fringe near the quadrature is linear to the amount of absorption. By calibrating the change in the interference pattern with an absorption standard, the aerosol absorption can be subsequently quantified. Other resources detailing the principles of the photothermal interferometric technique are provided by Owens et al. Bialkowski, and Davis and Petuchowski [2,10–12].

3. Apparatus

A Mach–Zehnder interferometer was built to create interference patterns as shown in Fig. 1. Two mirrors and two beam splitters are used to construct the reference beam and the probe beam. A coherent sensing beam emitted from a frequency stabilized He-Ne laser was divided by the 1st beam splitter. Half of the beam was transmitted through the 1st beam splitter and the other half of the beam was reflected at the 1st mirror with an angle of 90°. The transmitted beam at the 1st beam splitter constructed a reference beam, which was reflected at the 2nd mirror with an angle of 90° and then continued toward the 2nd beam splitter. The 90° reflected beam at the 1st mirror constructed a probe beam, which was recombined with the reference beam at the 2nd beam splitter. The two beams recombined at the 2nd beam splitter created an interference pattern. Then, an Ar-ion CW laser (Innova 90, Coherent) with the wavelength of a 514 nm was used as a pump laser in an off-axis configuration using two rectangular prisms, as shown in Fig. 1. The beam diameter of the He-Ne laser was approximately 0.5 mm and that of the Ar-ion green laser was approximately 1.5 mm. The beam profiles for both lasers were observed to be TEM_{00}. The green laser beam overlapped the He-Ne probe beam; the overlapping length was adjusted to approximately 50 mm.

The green laser beam was modulated at 200 Hz using a mechanical chopper (SR-540, Stanford Research Systems). The modulated green laser heated up the aerosol sample, so that the refractive index surrounding the sample at the probe beam was altered. The dissipation of the spectrally absorbed energy created a temperature gradient near the center of the probe beam. Then, the localized heating created a refractive index gradient surrounding the particles. When the probe beam takes a slightly different *optical* path length relative to the reference beam, interference pattern shifts due to the difference in the *optical* path lengths between the two beams. The interference patterns were recorded at 30 frames per second (fps) using a CCD camera (SCC-B2331, Samsung). The CCD camera consisted of a Sony 470 K pixels 1/3" super HAD-IT CCD module. The images were transferred to PC through a graphics processing unit. The interference images were saved every 1 s before image analysis. The time resolution for this system was 1 s. The image was converted into intensity data. All the optical components and sample cell were surrounded by a rectangular enclosure made with acrylic box. Sound-absorbing materials attached inside the enclosure block the propagation of sound wave that could affect the interference patterns. We waited for 5 min after loading the aerosol particles, and then collected 60 images for 1 min. The tube from our atomizer to the sample cell was about 2 meter long and the inner diameter of the tube was 4 mm. Then, the volume of the tube was calculated to be approximately 25 cm^3. The cross sectional area of the tube was 0.126 cm^2. The volume flow rate of aerosol was set to 0.15 lpm, which is 2.5 cm^3/s. The flow velocity inside the tube was calculated by dividing the volume flow rate by the cross sectional area, resulting in about 20 cm/s. Therefore, it took about 10 s for the aerosol to reach the sample cell after being injected from the atomizer. A time delay of 10 s was believed to have been experienced in the beginning of flow. However, once the tube was completely filled with the aerosols, the instrument exhibited an immediate response to the aerosol sample.

Aerosols were injected into the sample cell at 0.15 lpm. Taking into account the flow rate, we ensured that the flow inside the sample cell remained laminar since the Reynolds number (Re) was less than 2300. Re is defined as the uD_h/ν, where u is the flow velocity, D_h is the hydraulic diameter of a rectangular duct and ν is the kinematic viscosity of the aerosol. The kinematic viscosity of the aerosol was assumed to be the same as that of air at 20 °C. The kinematic viscosity of the air at 20 °C is 15×10^{-6} m^2/s. We used a rectangular typed sample cell. The cross section for this sample cell was 90 mm × 10 mm. The Re for the rectangular sample cell was calculated to be 240 which was much smaller than 2300. Therefore, the flow inside the sample was thought to still be laminar. We performed a 2-D numerical analysis for our sample cell consisting of a 12 mm wide aerosol sample inlet. The flow inside our sample cell remained laminar as shown in Fig. 2.

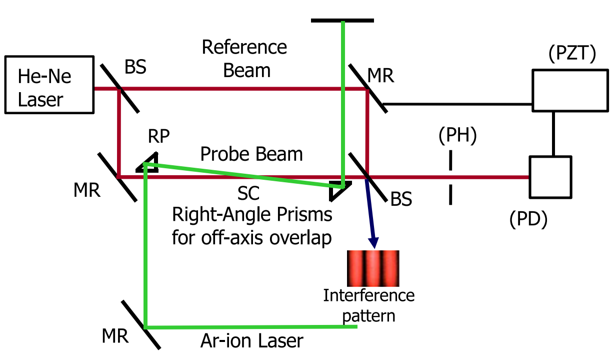

Fig. 1. Schematic of the Mach–Zehnder interfermetric optical configuration. (Parentheses given with PH, PD and PZT indicate that those components are not used in the current setup but will be used for upgrade. See more details in results and discussion.).

4. Results and discussion

A typical interference pattern created in our Mach–Zehnder interferometer is shown in Fig. 3a. The constructive interference pattern can be clearly distinguished from the destructive interference pattern. The thickness and spacing of the fringe depend on the alignment of both the reference beam and the probe beam. The thickness of fringe became narrow when the probe beam was recombined off-axis from the center of the reference beam. In the present study, the thickness and the spacing between the fringes was fixed to a specific position at which the sensitivity of the signal was maximized.

The level of brightness of the interference pattern was analyzed using free software (ImageJ, http://rsb.info.nih.gov/ij/download.html) in order to quantify the change of the interference pattern. The intensity of the interference image was obtained by processing the region of interest (ROI) along the horizontal center line of the image. Then, the image was converted into a graph, as